LAWRENCE
LIVERMORE
NATIONAL
LABORATORY

# Nuclear Forensic Analysis of Uranium Oxide Powders Interdicted in Victoria, Australia

M. Kristo, E. Keegan, M. Colella, R. Williams, R. Lindvall, G. Eppich, S. Roberts, L. Borg, A. Gaffney, J. Plaue, K. Knight, E. Loi, M. Hotchkis, K. Moody, M. Singleton, M. Robel, I. Hutcheon

February 29, 2016

**Disclaimer**

This document was prepared as an account of work sponsored by an agency of the United States government. Neither the United States government nor Lawrence Livermore National Security, LLC, nor any of their employees makes any warranty, expressed or implied, or assumes any legal liability or responsibility for the accuracy, completeness, or usefulness of any information, apparatus, product, or process disclosed, or represents that its use would not infringe privately owned rights. Reference herein to any specific commercial product, process, or service by trade name, trademark, manufacturer, or otherwise does not necessarily constitute or imply its endorsement, recommendation, or favoring by the United States government or Lawrence Livermore National Security, LLC. The views and opinions of authors expressed herein do not necessarily state or reflect those of the United States government or Lawrence Livermore National Security, LLC, and shall not be used for advertising or product endorsement purposes.

# Nuclear Forensic Analysis of Uranium Oxide Powders Interdicted in Victoria, Australia

M. Kristo*[1], E. Keegan[2], M. Colella[2], R. Williams[1], R. Lindvall[1], G. Eppich[1], S. Roberts[1], L. Borg[1], A. Gaffney[1], J. Plaue[1], K. Knight[1], E. Loi[2], M. Hotchkis[2], K. Moody[1], M. Singleton[1], M. Robel[1], I. Hutcheon[1]

[1]Lawrence Livermore National Laboratory, P.O. Box 808, L-186, Livermore, CA 94551, USA

[2]Australian Nuclear Science and Technology Organisation, Locked Bag 2001, Kirrawee, NSW 2232, Australia

**Abstract.**

Nuclear forensic analysis was conducted on two uranium samples confiscated during a police investigation in Victoria, Australia. The first sample, designated NSR-F-270409-1, was a depleted uranium powder of moderate purity ($\sim 1000$ µg/g total elemental impurities). The chemical form of the uranium was a compound similar to $K_2(UO_2)_3O_4\cdot 4H_2O$. While aliquoting NSR-F-270409-1 for analysis, the body and head of a Tineid moth was discovered in the sample. The second sample, designated NSR-F-270409-2, was also a depleted uranium powder. It was of reasonably high purity ($\sim 380$ µg/g total elemental impurities). The chemical form of the uranium was primarily $UO_3\cdot 2H_2O$, with minor phases of $U_3O_8$ and $UO_2$. While aliquoting NSR-F-270409-2 for analysis, a metal staple of unknown origin was discovered in the sample. The presence of $^{236}U$ and $^{232}U$ in both samples indicates that the uranium feed stocks for these samples experienced a neutron flux at some point in their history. The reactor burn-up calculated from the isotopic composition of the uranium is consistent with that of spent fuel from natural uranium (NU) fueled Pu production. These nuclear forensic conclusions allow us to categorically exclude Australia as the origin of the material and greatly reduce the number of candidate sources.

---

* Correspondence author (e-mail: kristo2@llnl.gov)

| Author | Title | File Name | Date | Page |
|---|---|---|---|---|
| M. Kristo*, E. Keegan2, M. Colella2, R. Williams1, R. Lindvall1, G. Eppich1, S. Roberts1, L. Borg1, A. Gaffney1, J. Plaue1, K. Knight1, E. Loi2, M. Hotchkis2, K. Moody1, M. Singleton1, M. Robel1, I. Hutcheon1 | Nuclear Forensic Analysis of Uranium Oxide Powders | 809404-1242360.docx | 29.02.2016 | 1 (25) |

**Keywords:**

Nuclear Forensics , Origin Assessment, Scanning Electron Microscopy (SEM), X-ray Diffraction , Inductively Coupled Plasma Mass Spectrometry, Depleted Uranium

# Introduction

On April 1, 2009, police in Victoria, Australia carried out a series of eight drug raids. According to The Age newspaper, police found a working amphetamine laboratory in a house in the suburbs of Melbourne, and unexpectedly found two containers of uranium material at a storage property in a nearby town. A team from the Victorian Department of Human Services, wearing special protective gear, was called in to remove the uranium and take it to a safe facility. A man was arrested in relation to the raid, but refused to say why he had hidden the uranium or for what purpose he had obtained the radioactive material [1, 2].

Within a week, the seizure had reached the attention of the Australian national legislature. Questions were asked about the quantity, chemical form, and isotopic composition of the seized material. In addition, the origin of the material – whether it had originated in Australia or not, whether it might have been from an existing or defunct mine, and whether it was related to previous seizures of material was of particular interest [3]. These are specifically the types of questions that the fledgling science of nuclear forensics seeks to answer [4,5]. Nuclear forensics has been defined as "*the analysis of intercepted illicit nuclear or radioactive material and any associated material to provide evidence for nuclear attribution. The goal of nuclear forensics analysis is to identify forensic indicators in interdicted nuclear and radiological samples or the surrounding environment, e.g., the container or transport vehicle. These indicators arise from known relationships between material characteristics and process history.*"[6]

Both uranium materials were subsequently delivered to the Australian Nuclear Science & Technology Organization (ANSTO) in Lucas Heights, Australia, as legal evidence. There, ANSTO scientists applied the techniques of nuclear forensics to answer the questions asked by Australian politicians, as well as the case agents of the Victoria Police. Subsequent to its initial analysis, ANSTO sent aliquots of the seized material to Lawrence Livermore National Laboratory (LLNL) in November 2010. They requested that LLNL conduct its own analysis, as part of an ongoing collaboration in nuclear forensics, to provide confirmation of ANSTO's results, and additional information where possible.

This paper describes the investigation and characterization conducted on the seized samples by both laboratories to determine their origin and history.  In addition to providing specific information in support of law enforcement and national security, this investigation serves as a real example of international engagement in nuclear forensics.  International scientific engagement in nuclear forensics, whether conducted in a multilateral setting, such as through the Nuclear Forensics International Technical Working Group (ITWG) [7,8], or in a bilateral, country-to-country setting, such as this investigation, serves to drive the standardization of methods, techniques, standards, and reference materials for nuclear forensics.  International collaborations such as this are absolutely crucial for developing and testing the comparability of nuclear forensic data acquired by different countries.

# Experimental

## Investigated Samples

Two different materials were received at ANSTO (Figure 1): 42.9 g of a bright yellow powder, which was given the tracking number NSR-F-270409-1, and 48.6 g of a dark green powder, which was given the tracking number NSR-F-270409-2.  Some months later, approximately 5 g aliquots of each material were sent to LLNL in plastic, screw-top vials. The samples (Figure 2) were given separate sample tracking numbers internal to LLNL, but, for ease of reference, the ANSTO tracking numbers are used throughout this paper.



**Fig. 1**. Interdicted samples received at ANSTO.
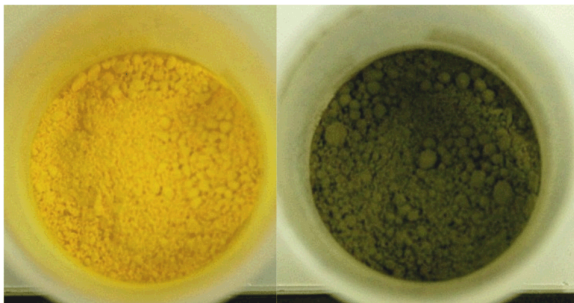Left:  NSR-F-270409-1 (42.9 g).  Right: NSR-F-270409-2 (48.6 g).

| Author | Title | File Name | Date | Page |
|---|---|---|---|---|
| M. Kristo*, E. Keegan2, M. Colella2, R. Williams1, R. Lindvall1, G. Eppich1, S. Roberts1, L. Borg1, A. Gaffney1, J. Plaue1, K. Knight1, E. Loi2, M. Hotchkis2, K. Moody1, M. Singleton1, M. Robel1, I. Hutcheon1 | Nuclear Forensic Analysis of Uranium Oxide Powders | 809404-1242360.docx | 29.02.2016 | 3 (25) |

**Fig. 2.** Close up of sample material as received at LLNL.
Left: NSR-F-270409-1. Right: NSR-F-270409-2.

## Analytical Procedures

Both ANSTO and LLNL conducted their analyses in accordance with the Nuclear Forensics International Technical Working Group's (ITWG's) Model Action Plan, which provides for 24-hour, 1-week, and 2-month reporting of results [9].

## Whole sample gamma spectrometry

High resolution gamma-ray spectroscopy was performed on the samples received at ANSTO using a Canberra instrument with a lead shielded precision planar HPGe detector. The acquisition period was 12 hours and the resulting spectrum was analyzed using the 'multi-group analysis for uranium (MGAU)' software package to determine the uranium isotopic abundance.

LLNL performed gamma spectrometry on approximately half of the mass of its samples (~ 2.5 g) using in-house HPGe gamma spectrometers. Spectra were acquired for 8 hours for initial categorization, and then 3 days for confirmation. All spectra were analyzed using an in-house version of the GAMANAL software. The sample aliquots analyzed by gamma spectrometry were subsequently used for most of the non-destructive tests (X-ray fluorescence (XRF), X-ray diffraction (XRD) and scanning electron microscopy (SEM)).

## Actinide isotopic and age-dating analysis

Both laboratories performed loss-on-heating experiments. At LLNL, sub-samples of approximately 2 g were dried at 140 °C for 2 hours; at ANSTO, sub-samples were dried at 110 °C for 3 hours. The masses of the samples were measured before and after heating to determine loss-on-heating, which should represent the moisture content (unbound $H_2O$) of the samples. At LLNL, additional aliquots of each sample were dried first at 140 °C for 2 hours, then at 750 °C for 12 hours, to look for mass or color

| Author | Title | File Name | Date | Page |
|---|---|---|---|---|
| M. Kristo*, E. Keegan2, M. Colella2, R. Williams1, R. Lindvall1, G. Eppich1, S. Roberts1, L. Borg1, A. Gaffney1, J. Plaue1, K. Knight1, E. Loi2, M. Hotchkis2, K. Moody1, M. Singleton1, M. Robel1, I. Hutcheon1 | Nuclear Forensic Analysis of Uranium Oxide Powders | 809404-1242360.docx | 29.02.2016 | 4 (25) |

changes indicative of chemically bound species, such as waters of hydration.

Isotopic analyses of uranium and plutonium were performed at LLNL by multi-collector inductively-coupled plasma mass spectrometry (MC-ICP-MS, Nu Plasma HR, Nu Instruments, Oxford, United Kingdom). Aliquots of the powders dried only at 140 °C were dissolved in $HNO_3/HF$. Gravimetric dilutions of the resulting solutions were spiked with [233]U, purified using UTEVA (Eichrom Technologies) resin, and then analyzed by MC-ICP-MS for total uranium content (by isotope dilution mass spectrometry (IDMS)) and uranium isotopic content. Aliquots of the powders dried at both 140 °C and 750 °C were also dissolved. Aliquots of secondary gravimetric dilutions of these solutions were spiked with [244]Pu, purified using anion exchange resin (AG1x8, 100-200 mesh) and TEVA resin (Eichrom Technologies), and then analyzed by MC-ICP-MS for total Pu content (by IDMS) and Pu isotopic content.

At ANSTO, the samples were analyzed in triplicate using an Elan6000 quadrupole ICP-MS (Perkin-Elmer Sciex Instruments) optimized for uranium isotopic measurement. A certified uranium oxide isotopic standard (NBL CRM 129-A) was used to correct for mass discrimination. Isotopic analysis of the samples was also performed at ANSTO by accelerator mass spectrometry (AMS). As the major isotopes were already determined by ICP-MS, only the isotopes [234]U and [236]U were measured using the AMS system. The [236]U/[234]U ratio of each sample was measured relative to those of the standard reference material NBL U030 and an internal standard (Aldrich AAA standard), the latter being used as a consistency check. The standard reference material NIST 4321C was used to determine the [236]U background level. Samples were prepared for AMS by adding iron nitrate solution (equivalent to 5 mg iron) to a 1 g aliquot of the dissolution used for ICP-MS (uranium concentration of approximately 50 μg/g). Uranium and iron were co-precipitated from this solution by addition of ammonium hydroxide. The precipitate was calcined at 900 °C to create hematite doped with uranium. This powder was mixed with a similar mass of niobium powder and inserted into AMS ion source target holders. Two targets for each of the two samples were prepared in this way. Each sample was measured three times and the results averaged to derive final results. The duplicate targets were measured once each as a consistency check. All results were consistent within measurement uncertainties and the background level was found to be negligible with reference to the samples and standards

Age dating was performed at LLNL using both the [234]U/[230]Th and [235]U/[231]Pa chronometers. Dissolutions of both samples were spiked with [229]Th and [233]Pa. U, Th, and Pa were then radiochemically separated, purified, and measured by MC-ICP-MS (Nu Plasma) for [230]Th and [231]Pa

| Author | Title | File Name | Date | Page |
|---|---|---|---|---|
| M. Kristo*, E. Keegan2, M. Colella2, R. Williams1, R. Lindvall1, G. Eppich1, S. Roberts1, L. Borg1, A. Gaffney1, J. Plaue1, K. Knight1, E. Loi2, M. Hotchkis2, K. Moody1, M. Singleton1, M. Robel1, I. Hutcheon1 | Nuclear Forensic Analysis of Uranium Oxide Powders | 809404-1242360.docx | 29.02.2016 | 5 (25) |

content [10, 11].  The concentrations of $^{230}$Th relative to $^{234}$U and of $^{231}$Pa relative to $^{235}$U were used to calculate model ages.

## Trace elemental analysis

Both laboratories performed X-ray fluorescence (XRF) analysis of each sample.  ANSTO analyzed pressed powders of NSR-F-270409-01 and -02 (approximately 4 g of material for each sample) using a Philips PW 2400 wavelength dispersive X-ray fluorescence spectrometer (XRF) fitted with a 2.7 kW, 60 kV Rh anode X-ray tube. Semi-quantitative elemental weight compositions were analyzed using the Uniquant™ software program.  LLNL performed XRF analyses using a Bruker S8 Tiger 4kW WD-XRF fitted with a Rh X-ray tube. Measurements were performed on loose powders loaded into sample cups with an 8 mm orifice and a 12 μm polypropylene film. Approximately 0.5 g of sample was used, which provided enough material to exceed theoretical infinite thickness for all elements (>30 μm). In order to measure all elements from Na to U, X-ray tube parameters varied from 30 to 60 kV and 67 to 135 mA. The crystal XS-55 (W/Si multilayer, 2d = 5.5 nm) was used to measure Na and Mg, and the crystal PET (pentaerythrite, 2d = 0.874 nm) was used to measure Al, Si, P, S, and Cl. All other elements were measured using the crystal LiF200 (lithium fluoride, 2d = 0.403 nm). Semi-quantitative elemental weight concentrations were calculated using the Bruker Quant-Express™ software package. Typical detection limits varied from approximately 50 to 500 μg/g.

LLNL also digested three 100 mg aliquots of each solid sample in concentrated nitric acid with 0.3% HF.  The resulting solutions were diluted in a $HNO_3$/HF solution (18% $HNO_3$ and 0.054% HF) to U concentrations of ~180 μg/g and analyzed by quadrupole inductively coupled plasma mass spectrometry (Q-ICPMS) (Thermo Electron X7).  An In internal standard was added to the solutions (5 ng/g) to correct for instrument drift and suppression from the uranium matrix.

## Sr and Pb isotopic analysis

LLNL routinely analyzes uranium ores and ore concentrates for Sr, Nd, and Pb isotopic composition for insight about provenance.  For these samples, the Nd concentration was too low for accurate isotopic measurement, so only Sr and Pb were analyzed. First, the samples were digested and then dried down on hot plates and under a heat lamp in a class 100 clean laboratory.  Then, uranium was adsorbed on anion exchange resin from 9 M HCl.  The wash through this column contains all the elements of interest: Th, Pb, the rare earths (neodymium), the alkaline earths (strontium), plus others, and is denoted as the Th-plus fraction.  U was then recovered by washing it from the resin with 0.1 M

HCl.  Th is removed from the Th-plus fraction by sorption on anion exchange resin from 8 M $HNO_3$.  The wash through this column contains Pb, Nd, Sr, plus others, and is denoted as the Pb-plus fraction.  The Th was recovered by washing it from the resin with 0.1 M HCl+0.005 M HF solution.  Th was purified further by passing it through a small anion resin bed in 9 M HCl (like the first column) to separate it from any residual U.  Lead was purified from the Pb-plus fraction by sorption on anion exchange resin from 1.8 M HCl, and the wash through this column contains the Nd and Sr.  Pb was recovered by washing it from the resin with 6 M HCl.  The Pb was sufficiently pure at this stage for measurement by MC-ICPMS.  Strontium was purified from the 1.8M HCl wash of the Pb-column using Eichrom Sr-spec™ resin

Sr was analyzed by thermal ionization mass spectrometry (TIMS, Thermo Element Triton).  Strontium masses [84]Sr, [86]Sr, [87]Sr, and [88]Sr were measured on Faraday cups.  All sample results were corrected for mass bias (instrument fractionation) using [86]Sr/[88]Sr = 0.1194.  Pb was analyzed by HR MC-ICP-MS (Nu Plasma).  Pb isotopes [204]Pb, [206]Pb, [207]Pb, and [208]Pb were measured using Faraday cups.  Pb isotopic results were corrected for mass bias using Tl added to the sample immediately prior to mass spectrometry analysis, using a [205]Tl/[203]Tl value of 2.3875.  Pb isotope ratios were all normalized to NBS 981.

## Light stable isotope analysis

LLNL's high vacuum fluorination system (HVFS) was used in the analysis of oxygen isotope ratios of the uranium samples.  The HVFS uses $ClF_3$ to liberate oxygen gas, which is then converted to $CO_2$ and analyzed with a GV Prism III gas source mass spectrometer [12] for O-isotopic composition and concentration. A low enriched uranium (LEU) working standard for uranium oxide (CRM-125A) has been established in order to improve the accuracy of O-isotope measurements of U material.  The isotopic composition of this material was referenced to two international standard reference materials (NBS28 and NBS030).  Elemental compositions for C, S, and N were determined using high-temperature pyrolysis followed by gas analysis (Elementar Vario PyroCube EA). Samples were combusted at 1020 °C over tungsten oxide in a continuous stream of helium carrier gas to produce $SO_2$, $N_2$ and $CO_2$ from any sulfur, nitrogen and carbon present in the sample. The resulting gases were then purified and quantified using a thermal conductivity detector (TCD).

## X-ray diffraction

Each laboratory also performed X-ray diffraction (XRD) on each sample.  At ANSTO, the X-ray diffraction spectra were collected using a Siemens Kristalloflex D500, with weighted Co K-alpha radiation (0.1789/0.17929 nm), in the

angular range 0.087-1.309 mrad, a step size of 0.35 mrad with a counting time of 20 seconds per point. The XRD patterns were analysed for phase composition using the X'Pert HighScore Pro™ package from Panalytical with reference to the powder diffraction file database of standards.  LLNL performed XRD on its samples using a Bruker D8 Discover MR XRD on a portion of the gamma spectrometry aliquot.

## Scanning electron microscopy (SEM)/X-ray energy dispersive spectrometry (EDS)

At ANSTO scanning electron microscopy specimens were prepared by mounting small fragments of samples onto carbon planchets, then overcoating them with a 5 nm layer of carbon to prevent electron charge build up. Samples were examined using a JEOL JSM-6400 SEM equipped with a Noran Voyager energy dispersive X-ray microanalysis system. Samples for transmission electron microscopy – electron energy loss spectroscopy (TEM-EELS) work were prepared by crushing small fragments of samples with analytical grade ethanol using mortar and pestle. A drop of the suspension was pipetted onto a lacy carbon film supported by a copper grid (200 mesh). TEM analysis was carried out using a JEOL 2010F field emission gun microscope operating at 197 kV and equipped with a Noran System Six energy dispersive X-ray microanalysis system.  At LLNL, each of the powders was analyzed using an FEI Inspect F SEM for scanning electron microscopy with X-ray energy dispersive spectrometry (SEM/EDS). Samples were prepared for SEM/EDS analysis by one of two methods:  surface transfer of the as-received sample or ultrasonication in solvent to promote disaggregation of the material, followed by transfer to a carbon planchet.

## Extraneous Objects

While aliquoting sample NSR-F-270409-1, an anomalous object, long and narrow in shape and fibrous in appearance (Figure 3) was discovered.  The object was separated from the bulk sample, placed in a small glass vial, and a separate chain-of-custody tracking number was initiated.  A quick, initial investigation using an optical microscope showed that the object had some similarity to an insect, albeit without its head.  A thorough examination of NSR-F-270409-1 was then conducted to determine if any additional objects could be found.  One other object with an appearance similar to an insect's head was located.  This new object was also separated from the sample aliquot, placed in a small glass vial, and a separate chain-of-custody was initiated.
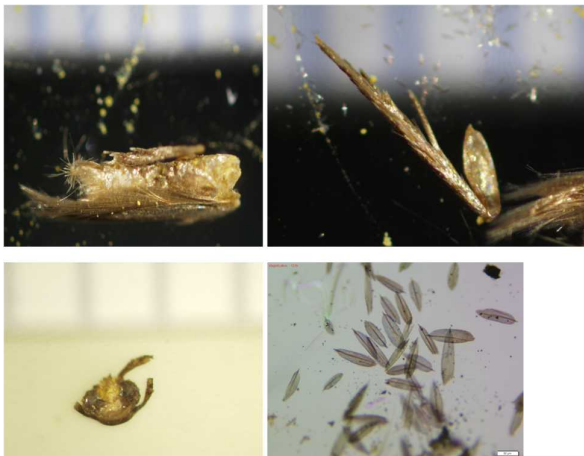
**Fig. 3.** Moth's body (top left) and detached leg (top right). Insect head (bottom left) and moth scales (bottom right). Out-of-focus mm scale can be seen in the background of top and bottom left images.

Similarly, while aliquoting sample NSR-F-270409-2, what appeared to be a metal staple (Figure 4) was discovered. The object was isolated, placed in a small glass vial, and a separate chain-of-custody initiated. Additional investigation of this sample did not yield any other extraneous objects. Further investigation of the objects isolated from both samples was later conducted using more advanced microscopy techniques.
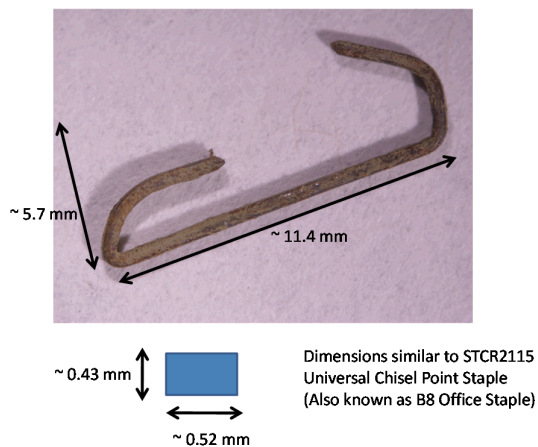


**Fig. 4.** Appearance and dimensions of staple found in NSR-F-270409-2. The blue box shows the cross-sectional dimensions of the staple.

| Author | Title | File Name | Date | Page |
|---|---|---|---|---|
| M. Kristo*, E. Keegan2, M. Colella2, R. Williams1, R. Lindvall1, G. Eppich1, S. Roberts1, L. Borg1, A. Gaffney1, J. Plaue1, K. Knight1, E. Loi2, M. Hotchkis2, K. Moody1, M. Singleton1, M. Robel1, I. Hutcheon1 | Nuclear Forensic Analysis of Uranium Oxide Powders | 809404-1242360.docx | 29.02.2016 | 9 (25) |

# Results

## Whole Sample Gamma Spectrometry

Gamma spectrometry was performed for initial categorization (Table 1). Within 24 hours, each laboratory was able to determine that samples NSR-F-270409-1 and NSR-F-270409-2 both consisted primarily of depleted uranium ($^{235}$U less than natural abundance) whose feedstock had experienced a neutron flux at some point, as demonstrated by the presence of $^{232}$U. Other fission and activation products were below detection limits. In order to reduce the detection limits for some of the fission and activation products further, LLNL acquired gamma spectra for each of the sub-samples over 3 days. Although the detection limits for these analyses were lower than in the initial analysis, no new nuclides were detected.

**Table 1.** High resolution gamma-ray spectrometry results at 24 hours. Other fission and activation products, including $^{54}$Mn, $^{60}$Co, $^{106}$Ru, $^{125}$Sb, $^{137}$Cs, $^{144}$Ce, $^{152}$Eu and $^{182}$Ta were below detection limits. Uncertainties are 1 standard deviation, derived solely from counting statistics.

| | $^{235}$U/$^{238}$U | $^{234}$U/$^{238}$U | $^{226}$Ra/$^{238}$U | $^{239}$Pu/$^{238}$U | gU/g sample | $^{232}$U | $^{40}$K/$^{238}$U |
|---|---|---|---|---|---|---|---|
| NSR-F-270409-1 (LLNL) | 4.23E-3 ± 1.5 % | 2.71E-5 ± 10.8% | 9.4E-12 ±49% | < 5.5E-6 | 0.693 ± 5 % | Present | 7.3e-5 ± 20% |
| NSR-F-270409-1 (ANSTO) | 4.40E-3 ± 3.4 % | 3E-5 ± 33% | | | | | |
| NSR-F-270409-2 (LLNL) | 4.00E-3 ± 1.4% | 2.57E-5 ± 12.6% | 1.42E-11 ± 31% | < 5.3E-6 | 0.750 ± 5% | Present | < 1.2e-5 |
| NSR-F-270409-2 (ANSTO) | 4.77E-3 ± 2.7% | 4E-5 ± 25% | | | | | |

## Actinide isotopic and age dating analysis

The loss-on-heating results from both laboratories are listed in Table 2. Both laboratories found that NSR-F-270409-1 lost about 1 wt. % and NSR-F-270409-2 lost about 6 wt. % upon heating slightly above 100 °C. Most notably, LLNL found that both samples lost additional weight upon heating to 750 °C and that NSR-F-270409-1 changed color from bright yellow to orange.

| Author | Title | File Name | Date | Page |
|---|---|---|---|---|
| M. Kristo*, E. Keegan2, M. Colella2, R. Williams1, R. Lindvall1, G. Eppich1, S. Roberts1, L. Borg1, A. Gaffney1, J. Plaue1, K. Knight1, E. Loi2, M. Hotchkis2, K. Moody1, M. Singleton1, M. Robel1, I. Hutcheon1 | Nuclear Forensic Analysis of Uranium Oxide Powders | 809404-1242360.docx | 29.02.2016 | 10 (25) |

**Table 2.** Sample weight loss upon heating. Expanded uncertainties use a coverage factor of two (k=2).

| Laboratory | LLNL | ANSTO | LLNL | Color change |
|---|---|---|---|---|
| Temp | 140 °C | 110 °C | 750 °C | 750 °C |
| Sample ID | wt % | wt % | wt % (additional) | |
| NSR-F-270409-1 | 1.126(±0.073) | 1.01(±0.014) | 4.675(±0.073) | Yellow→Orange |
| NSR-F-270409-2 | 5.748(±0.051) | 6.09(±0.014) | 5.162(±0.055) | None |

The U assay and isotopic results, as determined by mass spectrometry, are summarized in Table 3. The results confirmed the initial gamma-ray spectrometry results; samples NSR-F-270409-1 and NSR-F-270409-2 were depleted uranium. Both samples also contained easily detectable amounts of $^{236}$U, consistent with the detection of $^{232}$U by gamma-ray spectrometry (both isotopes are products of reactor irradiation). The isotopic compositions of the two seized samples were clearly different, suggesting that they were derived from different source material. The $^{235}$U/$^{238}$U ratios provided depletion levels ($^{235}$U content) for NSR-F-270409-01 and NSR-F-270409-02 of ~0.44 at% and ~0.42 at% respectively. In the uranium enrichment process, the level of depletion of $^{235}$U in the tails is determined by the degree of stripping employed in the enrichment cascade, which is, in turn, an engineering decision made primarily for economic reasons. A larger stripping section makes more efficient use of the uranium feed, but at a greater capital cost. For example, historical depletion levels for U.S. enrichment plants were in the 0.2-0.3 at% range, although the U.S. Department of Energy holds substantial stocks of material with depletion levels consistent with these interdicted samples [13]. Historical depletion levels for Soviet enrichment plants were in the 0.3-0.4 at% range, but more recent depletion levels for Russian enrichment plants are lower [14]. Enrichment programs in other countries may also have depleted their uranium tailings to similar levels. The $^{236}$U concentrations in depleted uranium are a function of the amount of recycled (irradiated, then reprocessed) uranium introduced into the enrichment cascade. Again, recycling irradiated uranium makes efficient use of material, but at the expense of increased $^{232}$U and $^{236}$U in the product.

**Table 3.** Uranium assay and isotopic abundances from MC-ICP-MS at LLNL and uranium isotopic abundances via a combination of Q-ICP-MS ($^{234}U/^{238}U$ and $^{235}U/^{238}U$) and AMS ($^{236}U/^{238}U$) at ANSTO. Expanded uncertainties (EU) use a coverage factor of three (k=3).

| Sample ID | Atom Ratios | | | | | | On a dry weight basis | |
|---|---|---|---|---|---|---|---|---|
| | $^{234}U/^{238}U$ | EU | $^{235}U/^{238}U$ | EU | $^{236}U/^{238}U$ | EU | Total U g U / g-sample | EU |
| NSR-F-270409-1 (LLNL) | 0.00002768 | 0.00000018 | 0.0044439 | 0.0000087 | 0.00002312 | 0.00000012 | 0.7085 | 0.0027 |
| NSR-F-270409-1 (ANSTO) | 0.0000279 | 0.0000021 | 0.004449 | 0.0000057 | 0.0000246 | 0.0000015 | | |
| NSR-F-270409-2 (LLNL) | 0.00002509 | 0.00000015 | 0.0040974 | 0.0000081 | 0.00007711 | 0.00000039 | 0.7988 | 0.0037 |
| NSR-F-270409-2 (ANSTO) | 0.0000261 | 0.0000039 | 0.004196 | 0.0000054 | 0.0000817 | 0.0000073 | | |

The concentrations of $^{230}Th$ relative to $^{234}U$ and $^{231}Pa$ relative to $^{235}U$ were both used to calculate model ages (Table 4), based upon the assumption that all Th and Pa was removed from the sample at some point, and that the material remained a closed system afterwards (no loss or addition of Th or Pa except through U decay) (10, 11). Both sets of model ages estimate the time since last purification of the parent uranium nuclide from the daughter nuclide (assuming complete purification). Incomplete purification will produce ages that are older than the true date of the last chemical purification. For example, while there is good agreement between the chronometers for NSR-F-270409-1, the resulting model age suggests that the material predates the development of both nuclear reactors and uranium enrichment. This model age clearly does not represent the time of material production. Since we expect that the production of $UF_6$ for the enrichment process would effectively remove Th and Pa, the result is most likely due to contamination by other sources of Th and Pa subsequent to production. Although the model age of NSR-F-270409-2 is feasible, and could represent its time of production, one must remember that it might be biased high as well, through similar mechanisms.

| Author | Title | File Name | Date | Page |
|---|---|---|---|---|
| M. Kristo*, E. Keegan2, M. Colella2, R. Williams1, R. Lindvall1, G. Eppich1, S. Roberts1, L. Borg1, A. Gaffney1, J. Plaue1, K. Knight1, E. Loi2, M. Hotchkis2, K. Moody1, M. Singleton1, M. Robel1, I. Hutcheon1 | Nuclear Forensic Analysis of Uranium Oxide Powders | 809404-1242360.docx | 29.02.2016 | 12 (25) |

**Table 4.** Model ages calculated from $^{230}$Th and $^{234}$U and $^{231}$Pa and $^{235}$U isotope abundances. Expanded uncertainties (EU) use a coverage factor of two (k=2).

| Sample ID | Reference Date | Years Before Reference Date | EU (years) | Model Date | EU (days) |
|---|---|---|---|---|---|
| | | $^{230}$Th-$^{234}$U Model Age (years) | | | |
| NSR-F-270409-1 | 28-Jan-11 | 75.3 | 1.3 | 20-Oct-35 | 480 |
| NSR-F-270409-2 | 28-Jan-11 | 47.89 | 0.85 | 9-Mar-63 | 310 |
| | | $^{231}$Pa-$^{235}$U Model Age (years) | | | |
| NSR-F-270409-1 | 10-Nov-11 | 76.84 | 0.92 | 6-Jan-35 | 340 |
| NSR-F-270409-2 | 10-Nov-11 | 49.05 | 0.60 | 21-Oct-62 | 220 |

From MC-ICP-MS analysis of the separated Pu fraction, we found that NSR-F-270409-1 had $^{239}$Pu detectable at the 150 fg/g level, but no other detectable Pu isotopes. NSR-F-270409-2 had no detectable Pu.

## Trace elemental analysis

The trace element impurity results from ICP-MS analyses are summarized in Table 5. X-ray fluorescence (XRF) results are shown in Table 6. NSR-F-270409-1 had a greater total contribution of impurities than NSR-F-270409-2. ICP-MS analysis measured a matrix-level concentration of K (6.7 wt. %) in NSR-F-270409-1, which was confirmed by XRF (6.36 wt % at LLNL, 8.75% at ANSTO). ANSTO's XRF analysis also detected F (2.0 %) and Th (0.127%) in NSR-F-270409-1. The level of F was below the detection limit of LLNL's XRF instrument. The presence of F would suggest that the uranium was fluorinated at some point in its history. The differences in the detection of Th may be due to heterogeneity in the powder sample.

**Table 5.** Trace impurity analysis (ICP-MS). Results are expressed as µg/g sample as received (not dried). Expanded uncertainties (EU) use a coverage factor of two (k=2).

| Element | NSR-F-270409-1 (n=3) | EU | NSR-F-270409-2 (n=2) | EU |
|---|---|---|---|---|
| Na | 91 | 8 | 41 | 2 |
| Mg | 10.5 | 1.0 | 29.8 | 1.0 |
| Al | 25 | 2 | 19.3 | 1.1 |
| K | 67000 | 3000 | < 100 | --- |
| Ca | 120 | 30 | 58 | 14 |
| Ti | 4.3 | 0.6 | 1.5 | 0.3 |
| V | 1.2 | 0.3 | < 0.04 | --- |
| Cr | 30.2 | 1.7 | 5.5 | 0.3 |
| Mn | 16.8 | 1.0 | 1.07 | 0.18 |
| Fe | 445 | 20 | 55 | 4 |
| Co | 2.7 | 0.3 | 0.31 | 0.19 |
| Ni | 19.5 | 1.5 | 4.5 | 0.5 |
| Cu | 16.8 | 0.8 | 6.3 | 0.4 |
| Zn | 9.3 | 0.8 | 0.9 | 0.5 |
| Se | 9.3 | 0.6 | < 0.05 | --- |
| Rb | 9.8 | 0.6 | < 0.2 | |
| Sr | 6.6 | 0.4 | 0.62 | 0.16 |
| Y | 0 | 0.3 | < 0.01 | --- |
| Zr | 1.5 | 0.3 | < 0.4 | |
| Nb | 0.25 | 0.11 | <0.003 | --- |
| Mo | 1.6 | 0.3 | < 0.04 | |
| Cd | 26.2 | 1.5 | < 0.05 | --- |
| Sn | 14.0 | 0.9 | 0.77 | 0.17 |
| Sb | 0.6 | 0.3 | <0.05 | --- |
| Ba | 36.9 | 1.6 | 8.0 | 0.4 |
| La | 0.58 | 0.04 | < 0.05 | --- |
| Ce | 1.1 | 0.3 | < 0.02 | --- |
| Nd | 0.07 | 0.04 | < 0.01 | --- |
| W | 6.0 | 0.5 | < 0.1 | --- |
| Tl | 1.0 | 0.3 | < 0.01 | --- |
| Pb | 18.0 | 1.7 | 48 | 3 |

**Table 6.** Impurity analysis results (XRF). Results are expressed as weight percent as received (not dried). Uncertainties are approximately ±10 percent relative. ND- Not detected.

| Element | NSR-F-270409-1 | NSR-F-270409-1 | NSR-F-270409-2 | NSR-F-270409-2 |
|---------|---------|---------|---------|---------|
| Lab | LLNL | ANSTO | LLNL | ANSTO |
| Ca | 0.08 | -- | -- | 0.08 |
| F | ND | 2.0 | -- | -- |
| Fe | 0.10 | 0.05 | 0.05 | 0.02 |
| K | 6.4 | 8.8 | -- | -- |
| Mg | -- | 0.02 | -- | 0.04 |
| S | -- | -- | -- | 0.05 |
| Zn | 0.03 | -- | 0.03 | -- |
| Cu | 0.03 | -- | 0.03 | -- |
| Th | ND | 0.13 | -- | -- |
| U | 68 | 74 | 70 | 84 |

## Sr and Pb isotopic analysis

Although the isotopic composition of Sr and Pb can often be a diagnostic signature for uranium ores or ore concentrate, neither Sr nor Pb analysis proved to have diagnostic value for these particular samples. Table 7 shows the Sr isotopic results for the 2 interdicted samples. The $^{87}Sr/^{86}Sr$ ratio for NSR-F-270409-1 and NSR-F-270409-2 are unremarkable, similar to many other ores and ore concentrates that we have analyzed. The Pb ratios for NSR-F-270409-1 and NSR-F-270409-2 are shown in Table 8 and are consistent with common lead.

**Table 7.** Sr isotopic ratios measured using TIMS. Expanded uncertainties (EU) use a coverage factor of two ( k=2).

| | $^{87}Sr/^{86}Sr$ | EU | $^{84}Sr/^{86}Sr$ | EU |
|---|---|---|---|---|
| NSR-F-270409-1 | 0.709209 | 0.000010 | 0.056495 | 0.000004 |
| NSR-F-270409-2 | 0.708442 | 0.000052 | 0.056654 | 0.000032 |

**Table 8.** Pb isotopic ratios (MC-ICP-MS). Expanded uncertainty (EU) uses a coverage factor of two (k=2).

| | $^{208}Pb/^{204}Pb$ | EU | $^{207}Pb/^{204}Pb$ | EU | $^{206}Pb/^{204}Pb$ | EU | $^{208}Pb/^{206}Pb$ | EU | $^{207}Pb/^{206}Pb$ | EU |
|---|---|---|---|---|---|---|---|---|---|---|
| NSR-F-270409-1 | 36.648 | 0.026 | 15.4971 | 0.0086 | 17.2010 | 0.0092 | 2.13056 | 0.00044 | 0.90095 | 0.00011 |
| NSR-F-270409-2 | 35.852 | 0.026 | 15.4468 | 0.0089 | 16.1523 | 0.0091 | 2.21957 | 0.00046 | 0.95626 | 0.00012 |

## Light stable isotope analysis

The use of light stable isotopes forms one of the cornerstones of modern geochemistry [15-18], but this

technique has only recently been used to characterize nuclear materials [19]. The C, N, and S content of both samples were at, or below, detection limits for light stable isotope analysis. The results of the O analysis are shown in Table 9. The oxygen isotopic compositions of uranium ore concentrates are derived from the oxygen isotopic composition of the uranium ore and the chemicals and water used to process the ore into ore concentrate, but are also affected by the process itself, which may cause isotopic fractionation. A developed interpretive methodology for oxygen isotopics of uranium ores and ore concentrates and further processed uranium material does not yet exist. Because meteoric waters always have negative $\delta^{18}O$ values, but atmospheric oxygen has a highly positive $\delta^{18}O$ values, a positive $\delta^{18}O$ values in our sample would tend to indicate incorporation of some atmospheric oxygen or evaporated water at some point during the milling process. NSR-F-270409-1 had positive $\delta^{18}O$ value, indicating incorporation of at least some atmospheric O, while NSR-F-270409-2 had a slightly negative $\delta^{18}O$ value.

**Table 9.** Light element abundances and oxygen isotopic abundance (gas mass spectrometry). Uncertainties are 2 standard deviations.

| Sample | N (g/g sample) | C (g/g sample) | S (g/g sample) | O (g/g sample) | $\delta^{18}O$ sample (‰) |
|---|---|---|---|---|---|
| NSR-F-270409-1 | 0.0016±0.0006 | 0.0010±0.0002 | <0.0008 | 0.168±0.007 | +1.7±0.9 |
| NSR-F-270409-2 | <0.0008 | 0.0007±0.0004 | <0.0008 | 0.179±0.006 | - 2.1±0.9 |

## X-Ray diffraction (XRD)

Table 10 shows the closest identifications for phases within the 2 interdicted materials, as well as for the aliquot of NSR-F-270409-1 heated to 750 °C for 12 hours. LLNL found that the chemical form of NSR-F-270409-1 was a compound similar to $K_2(UO_2)_3O_4 \cdot 4H_2O$. The aliquot of NSR-F-270409-1 heated to 750 °C for 12 hours was identified as a mixture of $K_2U_4O_{13}$ and $K_2U_2O_7$. XRD at ANSTO suggested the likely composition of NSR-F-270409-01 was uranium ammonia oxide hydrate $(2UO_3.NH_3.3H_2O)$. LLNL found that the chemical form of NSR-F-270409-2 was primarily $UO_3 \cdot 2H_2O$, with minor phases of $U_3O_8$ and $UO_2$. ANSTO also found that NSR-F-270409-2 was identified as a mixed uranium oxide-hydrated, typically a combination of $U_aO_b$ and $UO_c.nH_2O$.

Each laboratory's interpretation of the XRD patterns was limited by the completeness of its library. The interpretations of the XRD pattern for NSR-F-270409-2 were essentially identical, because each library had patterns for the various forms of uranium oxide. The interpretations for NSR-F-270409-01 were somewhat different between the laboratories, primarily due to differences in their databases of XRD patterns. The closest match for NSR-F-270409-01 at LLNL was agrinierite, a mineral similar to

$K_2(UO_2)_3O_4 \cdot 4H_2O$, in which K, Ca, and Sr can serve as the cations interchangeably, while the closest match at ANSTO was uranium ammonia oxide hydrate, because ANSTO did not have an XRD pattern for agrinierite in their library. $K_2(UO_2)_3O_4 \cdot 4H_2O$ (7.6 wt. % K) is consistent with the presence of K at 6-7 weight %, while uranium ammonia oxide hydrate is not. However, neither XRD interpretation exactly matched the obtained pattern and this appears to be a highly unusual compound.

**Table 10.** Phase identification (XRD)

| Sample # | Major Phases | Minor Phases |
|---|---|---|
| NSR-F-270409-1 (LLNL) | $K_2(UO_2)_3O_4 \cdot 4H_2O$ (closest match) | $U_3O_7$ |
| NSR-F-270409-1 (ANSTO) | $2UO_3 \cdot NH_3 \cdot 3H_2O$ (closest match) | |
| NSR-F-270409-1 heated to 750 °C (LLNL) | $K_2U_4O_{13}$ | $K_2U_2O_7$ |
| NSR-F-270409-2 (LLNL) | $UO_3 \cdot 2H_2O$ | $U_3O_8$, $UO_2$ |
| NSR-F-270409-2 (ANSTO) | $UO_3 \cdot 2H_2O$ | $(UO2)_8O_2(OH)_{12} \cdot 12H_2O$ |

## Scanning electron microscopy (SEM)/ X-ray energy dispersive spectrometry (EDS)

Electron microscopy characterization clearly showed that particles from the two samples had very dissimilar morphologies. The observed morphology and agglomeration behavior of NSR-F-270409-1 (Figure 5) was similar to uranium oxides that have been prepared using a caustic precipitation process. Energy dispersive x-ray spectroscopy (EDS) confirmed the presence of F, K, Al, and C in the sample. The presence of 6-7 weight percent of potassium (as also confirmed through XRF and ICP-MS analysis) suggested the potential use of a potassium hydroxide precipitation. Thus, a comparison was made with an exemplar material produced in-house through precipitation of uranyl ions from solution using KOH (Figure 6). While the in-house reference material and NSR-F-270409-1 had similar morphologies, this general morphology is also somewhat consistent with descriptions provided in the literature of certain gas phase hydrolysis processes [20], and is not a unique identifier of process history. No foreign materials were observed during SEM analysis.
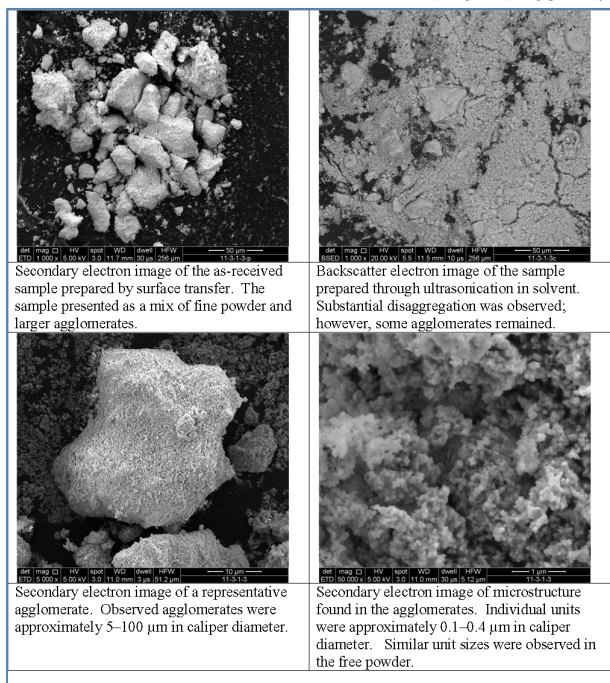
| Author | Title | File Name | Date | Page |
|---|---|---|---|---|
| M. Kristo*, E. Keegan2, M. Colella2, R. Williams1, R. Lindvall1, G. Eppich1, S. Roberts1, L. Borg1, A. Gaffney1, J. Plaue1, K. Knight1, E. Loi2, M. Hotchkis2, K. Moody1, M. Singleton1, M. Robel1, I. Hutcheon1 | Nuclear Forensic Analysis of Uranium Oxide Powders | 809404-1242360.docx | 29.02.2016 | 17 (25) |

Secondary electron image of the as-received sample prepared by surface transfer. The sample presented as a mix of fine powder and larger agglomerates.

Backscatter electron image of the sample prepared through ultrasonication in solvent. Substantial disaggregation was observed; however, some agglomerates remained.

Secondary electron image of a representative agglomerate. Observed agglomerates were approximately 5–100 μm in caliper diameter.

Secondary electron image of microstructure found in the agglomerates. Individual units were approximately 0.1–0.4 μm in caliper diameter. Similar unit sizes were observed in the free powder.

**Fig. 5.** SEM photomicrographs of NSR-F-270409-1.



**Fig. 6**. Secondary electron image of uranyl that has been precipitated using potassium hydroxide and dried to constant mass at 85°C. Note for comparison the scales are the same as the bottom images of Figure 5.

The morphology of NSR-F-270409-2 (Figure 7) did not completely match that displayed by material processed by methods LLNL has examined thus far. The irregularity in morphology suggests a solution-based precipitation over a gas phase process [21]. In addition, the faceted structure of many of the grains is often characteristic of heat exposure during processing. EDS indicated the presence of Si, C, and Al and, as for NSR-F-270409-1, no foreign materials were observed during SEM analysis.
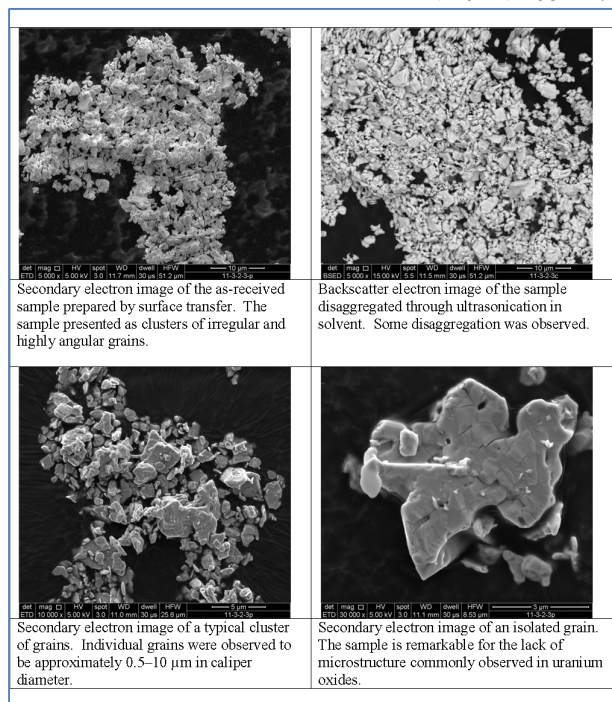
**Fig. 7.** SEM photomicrographs of NSR-F-270409-2.

The staple from NSR-F-270409-2 was also analyzed using SEM/EDS, performing EDS spot analyses at many points over the surface of the staple where contamination from the uranium oxide of the sample was minimal or absent. The morphology and angles of the chisel point were determined. One of the legs of the staple was then broken off, to allow analyses of the interior material. The staple core composition is dominated by Fe, with high and variable C, Al, and Mn. Higher O (10-30 wt%) and C (8-60 wt%) concentrations, and lower Fe concentrations (<40 wt%) were observed from the staple surface relative to the staple core, as well as higher Al (>15 wt%) and variable Sn. Small amounts of Si (~1 wt% and less) and trace amounts of S, Cl, K, Ca, Mn, Mg, and Cu were also observed across the staple surfaces.

# Discussion

## NSR-F-270409-1

Sample NSR-F-270409-1 is a depleted uranium powder of moderate purity (~1000 µg/g total elemental impurities). The chemical form of the uranium is a compound similar to $K_2(UO_2)_3O_4 \cdot 4H_2O$ (called "agrinierite" in its mineral form, in which combinations of K, Ca, and Sr can serve as the cations), which degrades to potassium uranium oxide ($K_2U_4O_{13}$) and potassium diruanate ($K_2U_2O_7$) upon heating. While we have not found any reference to the use or production of $K_2(UO_2)_3O_4 \cdot 4H_2O$ or a similar compound in

the literature, it is probably formed from the reaction of $UF_6$ with a KOH solution, similar to the production of ammonium diuranate (ADU) in the fuel conversion process. This would also account for the residual F observed through XRF and SEM/EDS analysis of the material. We also note that the morphology and XRD patterns for NSR-F-270409-1 are similar to a laboratory-synthesized exemplar, in which uranyl ions were precipitated using KOH, suggesting (but not confirming) a similar chemical composition and processing history.

The uranium feed stock for NSR-F-270409-1 has experienced a neutron flux as demonstrated by the presence of $^{232}U$ and $^{236}U$. However, the absence of detectable levels of activation (Pu) and fission products indicates that the irradiated material has been reprocessed. The levels of $^{232}U$ and $^{236}U$ in this sample are quite low, but consistent with burn-up levels typical for Pu production. Therefore, the uranium isotopic content of NSR-F-270409-1 is consistent with tails from an enrichment process, in which natural uranium (NU) fuel irradiated in a Pu production reactor was reprocessed and later used as feed (Figure 8). If we assume that the enrichment process used only the recycled NU fuel as feed, then, using a combination of reactor modeling (ORIGEN-ARP using an RBMK reactor model) and enrichment cascade modeling (a spreadsheet implementation of the De La Garza equations) [22-23], we can calculate that the Pu produced in the reactor would have a $^{240}Pu$ abundance of approximately 1.3-1.5%, a type of weapons-grade Pu often referred to as "ivory grade". Alternatively, the feed could have been a mixture of reprocessed NU fuel and unirradiated NU. In this case, the burnup of the irradiated NU fuel, and the $^{240}Pu$ abundance of the Pu produced, would have been correspondingly higher. The modeling process for these results is not very sensitive to assumptions of either reactor type or product enrichment. Unfortunately, this lack of sensitivity also means that we cannot use the same modeling approach to uniquely determine either reactor type or product enrichment.
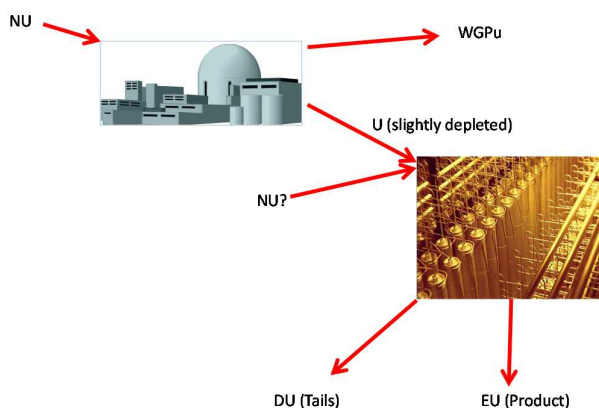


**Fig. 8.** Notional fuel cycle that produced depleted uranium (DU) for NSR-F-270409-1 & NSR-F-270409-2.

## NSR-F-270409-2

Sample NSR-F-270409-2 is a depleted uranium powder of reasonably high purity (~380 µg/g total elemental impurities). The chemical form of the uranium is primarily $UO_3\cdot 2H_2O$, with minor phases of $U_3O_8$ and $UO_2$. The uranium feed stock for NSR-F-270409-2 also experienced a neutron flux, and levels of $^{232}U$ and $^{236}U$ in this sample are also quite low and consistent with burn-up levels typical for Pu production. The U isotopic composition of NSR-F-270409-2 is consistent with tails from an enrichment process, in which natural uranium (NU) fuel irradiated in a Pu production reactor was reprocessed and used as feed (Figure 8). Using the same process employed with the results from NSR-F-270409-1, we calculated that the Pu produced in the reactor had a $^{240}Pu$ abundance of approximately 4.9-5.5 at%, which is higher than for NSR-F-270409-1, but still weapons grade. Alternatively, the feed for the enrichment process could have been a mixture of reprocessed NU fuel and unirradiated NU. In this case, the burn-up of the irradiated NU fuel, and the $^{240}Pu$ abundance of the Pu produced, would be correspondingly higher.

## Technical Conclusions Relevant to Attribution

Since Australia has never had a uranium reprocessing facility, we can categorically state that the material for both NSR-F-270409-1 and NSR-F-270409-2 originated outside of Australia. Depleted uranium has many legitimate uses, so it seems quite likely that the material was imported into Australia for legitimate purposes, but subsequently fell outside of legitimate control. The country of origin was an advanced nuclear state, producing weapons grade plutonium and enriching uranium using recycled reactor fuel. The depletion level of this material is typical of that produced in the former Soviet Union and also matches that of some (non-typical) US depleted uranium stocks. There may be other countries that have depleted uranium to these levels as well. The use of NU fueled Pu production reactors followed by reprocessing the U from the irradiated fuel as feed for an enrichment cascade was characteristic of many countries' nuclear programs, e.g., the former Soviet Union [24-25].

The 2013 Global Fissile Material Report [26] lists 7 countries with substantial stocks of both weapons grade plutonium and enriched uranium, although many of them may not have fuel cycles consistent with the isotopic composition of this material. An accurate age of the material would be extremely useful in ruling out certain of these countries as the countries of origin. We would expect that the enrichment process would effectively reset the $^{234}U$-$^{230}Th$ and $^{235}U$-$^{231}Pa$ chronometers. The model age of 75 years for NSR-F-270409-1, however, predates the era of Pu production and U enrichment, so the sample has most

| Author | Title | | File Name | Date | Page |
|---|---|---|---|---|---|
| M. Kristo*, E. Keegan2, M. Colella2, R. Williams1, R. Lindvall1, G. Eppich1, S. Roberts1, L. Borg1, A. Gaffney1, J. Plaue1, K. Knight1, E. Loi2, M. Hotchkis2, K. Moody1, M. Singleton1, M. Robel1, I. Hutcheon1 | Nuclear Forensic Analysis of Uranium Oxide Powders | | 809404-1242360.docx | 29.02.2016 | 21 (25) |

likely been contaminated with material that added excess $^{230}$Th and $^{231}$Pa (e.g., environmental natural uranium). Therefore, that age is not useful for nuclear forensic purposes. We noted that the model age of NSR-F-270409-2 of 48 years is feasible. If accurate (that is, if the sample remained uncontaminated after production), the early 1960's date would rule out all countries except the United States, Great Britain, and the Soviet Union as the source of the material. These were the only countries with both active Pu production and U enrichment at that time. Contamination of the original nuclear material with material that added excess $^{230}$Th and $^{231}$Pa (e.g., environmental natural uranium), however, cannot be ruled out.

## Moth in NSR-F-270409-1

Upon careful examination, the original object found in NSR-F-270409-1 was clearly the headless body of a moth (Figure 3, top left). One of the legs of the moth had become detached during transfer of the object from the powdered material to a glass vial as shown in Figure 3, top right. The additional object found in NSR-F-270409-1 was clearly an insect's head (Figure 3, bottom left), most likely the detached head from the moth body. Two entomologists examined the optical micrographs without reference to the source of the insect. Although the body was not intact, both experts expressed that it was most likely a moth from the family *Tineidae* (fungus moths or tineid moths). These types of moths form a massive and diverse group, but additional research is underway to identify the exact species and life stage of this moth. If the range of the species were limited to a specific region or set of regions, this identification might provide a valuable clue to the history of the material, in particular what route the material may have taken prior to its seizure, a so-called "route attribution" or "pathways" signature.

## Staple in NSR-F-270409-2

The object found in NSR-F-270409-2 was a used metal staple, highly corroded and covered with a layer of the native uranium oxide material comprising the bulk of the sample. The appearance and dimensions of the staple are shown in Figure 4. The dimensions of the staple are similar to, but not the same as, the STCR2115 and B8 office staples commonly found in many countries. We do not know how exposure to the unique environment of NSR-F-270409-2 might have affected the staple materials, but, overall, the staple appears to be crudely made compared to commercial staples available today. The C composition of our analyses was more consistent with a base material of high-carbon iron, rather than steel, which is more typically used for staples. The higher Al and variable Sn seen in the EDS

analysis was suggestive of a thin coating. If true, then the Cl might be a residual from $SnCl_3$ used for electroplating.

## Conclusions

Nuclear forensic analysis of the two seized samples was undertaken. Sample NSR-F-270409-1 was a depleted uranium powder of moderate purity (~71% U by weight). The chemical form of the uranium was a compound similar to $K_2(UO_2)_3O_4 \cdot 4H_2O$ and which degrades to potassium uranium oxide ($K_2U_4O_{13}$) and potassium diuranate ($K_2U_2O_7$) upon heating. In addition, we discovered the body and head of a Tineid moth in sample NSR-F-270409-1. Sample NSR-F-270409-2 was a depleted uranium powder of reasonably high purity (~80% U by weight). The chemical form of the uranium was primarily $UO_3 \cdot 2H_2O$, with minor phases of $U_3O_8$ and $UO_2$. In addition, we discovered a metal staple of unknown origin in this sample. The uranium feed stock for both samples had experienced a neutron flux as demonstrated by the presence of [232]U and [236]U. Other than the fact that NSR-F-270409-1 and NSR-F-270409-2 were seized at the same location and that they were both depleted uranium materials, they appear to be unrelated with respect to production method. However, they both are consistent with material from a country with current or historical weapons grade Pu production and U enrichment using reprocessed uranium from Pu production as feed for the enrichment process.

This work demonstrates the value of applying multiple methods to nuclear forensics problems, even though the results often do not serve as unique identifiers. This particular case also demonstrates how traditional forensics can work in tandem with radioactive material analysis to support nuclear forensic conclusions.

# References

1. Roberts, G.: "Uranium, drugs seized in Victorian raids," The Age, April 1, 2009, found at http://news.theage.com.au/breaking-news-national/uranium-drugs-seized-in-victorian-raids-20090401-9ju4.html on 12/13/12.

2. Silvester, J.: "Police on drugs raid find mysterious uranium stash," The Age, April 2, 2009, found at http://www.theage.com.au/national/police-on-drugs-raid-find-mysterious-uranium-stash-20090401-9jsq.html on 12/13/12.

3. Ludlam, S.: Question 1482 posed to the Minister representing the Attorney-General,http://parlinfo.aph.gov.au/parlInfo/search/display/display.w3p;query=Id%3A%22chamber%2Fhansards%2F2009-06-17%2F0263%22 on 12/13/12.

4. Moody, K., Hutcheon, I., Grant, P: Nuclear Forensic Analysis, Taylor & Francis, Boca Raton, FL, 2005.

5. Kristo, M.: Nuclear Forensics. In: Handbook of Radioactivity Analysis (M. F. L'Annuziata, ed.), 3rd ed. Elsevier, San Francisco, 2012.

6. IAEA: Nuclear Forensics Support, IAEA Nuclear Security Series No. 2, International Atomic Energy Agency, Vienna, 2006.

7. Niemeyer, S. and Koch, L.: The nuclear smuggling International Technical Working Group: Making a difference in combating illicit trafficking. In: Proceedings from the Conference on Advances in Destructive and Non-Destructive Analysis for Environmental Monitoring and Nuclear Forensics, Karlsruhe, Germany, October 21-23, 2002. International Atomic Energy Agency, Vienna, 2002, pp. 17-19.

8. Smith, D., Biro, T., Chartier, B., Mayer, K., Niemeyer, S., Thompson, P. Recent Activities of the Nuclear Smuggling International Technical Working Group to Thwart Illicit Trafficking. In: Proceedings of the IAEA Conference on Illicit Nuclear Trafficking, Edinburgh, Scotland, November 19-22, 2007. International Atomic Energy Agency, Vienna, 2007, pp. 289-296.

9. Smith, D., Kristo, M., Niemeyer, S., Dudder, G.: Documentation of a model action plan to deter illicit nuclear trafficking. J. Radioanal. Nucl. Chem. 276, 415 (2008).

10. Williams, R. and Gaffney A.: 230Th-234U model ages of some uranium standard reference materials. Proc. Radiochimica Acta, 1, 31 (2011).

11. Eppich, G., Williams, R., Gaffney, A., Schorzman, K.: 235U-231Pa age dating of uranium-rich materials for nuclear forensic investigations. Anal. At. Spectrom. 28, 666 (2013).

12. Borthwick, J., Harmon, R.: A note regarding the use of ClF3 as an alternative to BrF5 for oxygen isotope analysis. Geochim. Cosmochim. Acta 46, 1665 (1982).

13. Hertzler, T., Nishimoto, D.: Depleted Uranium Management Alternatives. EGG-MS-11416 (August 1994).

14. Bukharin, O.: Integration of the Military and Civilian Nuclear Fuel Cycles in Russia. Science in Global Security 4, 404 (1994).

15. Craig, H.: Isotopic variations in meteoric waters. Science 133, 1702 (1961).

16. Fayek, M., Kyser T.: Low temperature oxygen isotopic fractionation in the uraninite–UO3–CO2–H2O system. Geochim. et Cosmochim. Acta, 64:13, 2185 (2000).

17. Friedman, I., Redfield, A., Schoen, B., Harris, J.: The variation of the deuterium content of natural waters in the hydrologic cycle. Rev. Geophysics, 2, 177 (1964).

18. Gat, J.: Atmospheric water balance - The isotopic perspective. Hydrological Processes, 14, 1357 (2000).

19. Pajo, L., Mayer, K., Koch, L.: Investigation of the oxygen isotopic composition in uranium oxide compounds as a new property in nuclear forensic science. Fresenius J. Anal. Chem., 317, 348 (2001).

20. Andreev, E.I. et al., Russian Journal of Non-Ferrous Metals, 50:3, 281 (2009).

21. Plaue, J. Forensic Signatures of Chemical Process History in Uranium Oxides, Ph.D. Dissertation, University of Nevada Las Vegas, May 2013.

22. De La Garza, A., Garrett, G., Murphy, J.: Multicomponent isotope separation in cascades. Chem. Eng. Science 14, 188 (1961).

23. De La Garza, A.: A generalization of the matched abundance-ratio cascade for multicomponent isotope separation. Chem. Eng. Science 18, 73 (1963).

24. Kruglov, A.: The History of the Soviet Atomic Industry, Taylor & Francis, New York, 2002, p. 141.

25. Podvig, P.: Russian Strategic Nuclear Forces, MIT Press, Cambridge, MA, 2001, p. 80.

26. International Panel on Fissile Material: Global Fissile Material Report 2013, 7th annual report of the International Panel on Fissile Materials, 2013.